Journal of Chromatography B, 877 (2009) 3111–3117

Contents lists available at ScienceDirect

Journal of Chromatography B

journal homepage: www.elsevier.com/locate/chromb

Metabolomic study for diagnostic model of oesophageal cancer using gas chromatography/mass spectrometry

Hao Wu[a], Ruyi Xue[a], Chunlai Lu[b], Chunhui Deng[c], Taotao Liu[a], Huazong Zeng[d], Qun Wang[b,*], Xizhong Shen[a,*]

[a] Department of Gastroenterology, Zhongshan Hospital, Shanghai Medical College, Fudan University, Fenglin Road 180, Shanghai 200032, China
[b] Department of Thoracic Surgery, Zhongshan Hospital, Shanghai Medical College, Fudan University, Shanghai 200032, China
[c] Department of Chemistry, Fudan University, Shanghai 200433, China
[d] Shanghai Sensichip Infotech Co., Ltd., Shanghai 200433, China

ARTICLE INFO

Article history:
Received 13 May 2009
Accepted 29 July 2009
Available online 7 August 2009

Keywords:
Metabolomic profiling
Oesophageal cancer
Biomarker
Gas chromatography/mass spectrometry

ABSTRACT

The prognosis for oesophageal cancer is poor. Attempts have been made for the identification of biomarkers for early diagnosis. Metabolomic panel has been evaluated as potential candidate biomarkers. With gas chromatography/mass spectrometry (GC/MS) as a sensitive modality for metabolomics, various tissue metabolites can be detected and identified. We hypothesized that tissue metabolomic biomarkers may be identifiable and diagnostically useful for oesophageal cancer. We present a metabolomic method of chemical derivatization followed by GC/MS to analyze the metabolic difference in biopsied specimens between oesophageal cancer and corresponding normal mucosae obtained from 20 oesophageal cancer patients. The GC/MS data was analyzed using a two sample *t*-test to explore the potential metabolic biomarkers for oesophageal cancer. A diagnostic model was constructed to discriminate normal from malignant samples, using principal component analysis (PCA) and receiver–operating characteristic (ROC) curves. *t*-Test showed a total of 20 marker metabolites detected were found to be different with statistical significance ($P < 0.05$). The multivariate logistic analysis yielded a complete distinction between the two groups. The diagnostic model could discriminate tumors from normal mucosae with an area under the curve (AUC) value of 1. Our findings suggest that this assay may potentially provide a new metabolomic biomarker for oesophageal cancer.

© 2009 Elsevier B.V. All rights reserved.

1. Introduction

Cancer of the esophagus is the eighth most common cancer in the world, and survival of the patients is universally poor [1]. There are two major histologic types of oesophageal cancer, esophageal squamous cell carcinoma (ESCC) and adenocarcinoma. Their epidemiological features differ considerably. In China and other East Asia countries, more than 90% of cases are ESCC, while adenocarcinoma is more common in the United States and European countries [2,3]. The 5-year overall survival rates remain low and we cannot reliably predict the outcome before treatment [4]. To improve the survival, various approaches have been taken. Screening and surveillance in patients at risk have been advocated.

The current diagnostic, screening, and surveillance methods for oesophageal cancer, such as upper gastrointestinal (GI) endoscopy, barium oesophagram, non-endoscopy-based balloon cytology, and serology markers (such as CYFRA 21-1) [5], have certain limitations in their own ways. For example, CYFRA 21-1 is not useful as a screening or surveillance test for its low specificity and sensitivity, although it is easy to perform. Endoscopic screening and surveillance remain to be most commonly used, which rely on taking adequate biopsies of the oesophageal mucosa. The accuracy in tissue biopsy in the detection of cancer in those endoscopically abnormal mucosa have ranged from 25 to 60% [6]. In an effort to fill the knowledge gap, metabolomic profiling of tumors may provide a rapid and alternative means of exploring the potential biomarkers.

Metabolomics, defined as quantitative measurement of low-molecular-weight metabolites in an organism at a specified time under specific environmental conditions [7], has been shown to be an effective tool for disease diagnosis [8–10], biomarker screening [11–14], and characterization of biological pathways [15]. Metabolomics has become a powerful platform for studies associated with the biological metabolisms in a large of research area [16,17]. However, metabolomics has not been systematically evaluated in oesophageal cancer. We hypothesized that tissue metabolomic biomarkers may be identifiable and diagnostically useful for oesophageal cancer. The aim of the study was to profile biopsy specimens from oesophageal cancer and their corresponding normal mucosae in the same patients using gas

* Corresponding authors. Tel.: +86 21 64041990; fax: +86 21 65641740.
E-mail addresses: doctorwangqun@yahoo.com.cn (Q. Wang), shen.xizhong@zs-hospital.sh.cn (X. Shen).

1570-0232/$ – see front matter © 2009 Elsevier B.V. All rights reserved.
doi:10.1016/j.jchromb.2009.07.039

chromatography mass spectrometry (GC/MS) metabolomics following chemical derivatization.

2. Experimental

2.1. Materials and chemicals

Ribitol as an internal standard was purchased from Shanghai Intechem Tech. Co. Ltd. (Shanghai, China). Methanol (pesticide residue grade), Bis-(trimethylsilyl)–trifluoroacetamide (BSTFA) plus 1% trimethylchlorosilane (TMCS) and amino acid standard solution were purchased from Sigma–Aldrich (St Louis, MO, USA). All other chemicals and reagents were purchased from Ampu Company (Shanghai, China). Distilled water was produced by the Milli-Q ReagentWater System (Millipore, MA, USA).

2.2. Patient recruitment and sample collection

This prospective study was approved by the Ethics Committee of Zhongshan Hospital. Informed consent was obtained from all participants. Matched tumor and normal mucosae from the same patients with oesophageal cancer ($n = 20$) were obtained oesophagectomy surgery, consisting of 18 ESCC and 2 adenocarcinoma. The diagnosis was confirmed by histopathologic evaluation. None of the patients received neoadjuvant chemotherapy or radiation therapy prior to oesophagectomy. Fresh tumor tissue and corresponding normal esophageal mucosa were snap-frozen in liquid nitrogen during oesophagectomy, then stored at −80 °C until processing. Tumor specimens were carefully microdissected to ensure that at least 90% of the analyzed tissue containing cancer cells. Corresponding normal mucosae were taken at least 5–10 cm away from the edges of a tumor. The tumor stage, histology differentiation, and resection margin were determined by routine histopathological examination of H & E stained specimens by a blinded pathologist.

2.3. Specimen processing

For GC/MS analysis, 20 mg of tissue sample was transferred to a 15-mL glass centrifuge tube. One milliliter of a monophasic mixture of chloroform–methanol–water (2:5:2, v/v/v) and 100 μL ribitol (0.1 mmol L^{-1}) as an internal standard were added to each sample and the mixture was ultrasonicated at ambient temperature (24–28 °C) for 100 min and then vortex-mixed for another 2 min. The samples were subsequently centrifuged at 18,000 × *g* for 3 min and 0.8 mL of the supernatant was collected separately from each sample into a 15 mL test tube. The collected supernatant was concentrated to complete dryness in a Turbovap nitrogen evaporator at 50 °C for 30 min. A total of 100 μL of toluene, kept anhydrous with sodium sulfate, was added to each of the dried tissue extracts, vortex-mixed for 1 min and again evaporated to complete dryness in a Turbovap nitrogen evaporator in order to eliminate any trace of water which may interfere with GC/MS analysis. The dried samples were then derivatized to increase the volatility of polar metabolites by adding 100 μL of bis-(trimethylsilyl)–trifluoroacetamide (BSTFA) plus 1% trimethylchlorosilane (TMCS) to each sample. The samples were then vortex-mixed for 1 min and incubated at 70 °C for 30 min. After incubation, samples were again vortex-mixed for 1 min and then transferred to vials for GC/MS analysis [18–20].

2.4. GC/MS analysis

A 1 μL aliquot of derivatized sample was injected splitless into an Agilent 6980 GC system equipped with a 30.0 m × 0.25 mm i.d. fused-silica capillary column with 0.25-μm HP-5MS stationary phase (Agilent, Shanghai, China). The injector temperature was set at 250 °C. Helium was used as carrier gas at a constant flow rate of 1 mL min^{-1} through the column [11,21]. The column temperature was initially kept at 60 °C for 3 min and then increased to 140 °C at 7 °C min^{-1}, where it was held for 4 min and further increased at 5 °C min^{-1} to 300 °C where it remained for 1 min. The column effluent was introduced into the ion source of an Agilent 5973 mass selective detector (Agilent Technologies). The MS quadrupole temperature was set at 150 °C and the ion source temperature at 230 °C. Masses were acquired from m/z 50–800. The mass accuracy of the instrument was 0.1 atomic mass unit (amu). The acceleration voltage was turned on after a solvent delay of 180 s. GC/MSD ChemStation Software (Agilent, Shanghai, China) was used for auto-acquisition of GC total ion chromatograms (TICs) and fragmentation patterns. Each compound had a unique fragmentation pattern composed of a series of split molecular ions, the mass charge ratios and the abundance of which could be compared with a standard mass chromatogram in the NIST (National Institute of Standards and Technology) mass spectra library by the ChemStation Software. For each peak, the software will generate a list of similarities comparing with every substance within the NIST library. Peaks with similarity index more than 70% were assigned compound names, while those having less than 70% similarity were listed as unknown metabolites [18].

The chromatograms were subjected to noise reduction and peaks with intensity higher than threefold of the ratio of signal-to-noise (S/N) were recorded prior to peak area integration. The relative intensity of each signal is defined as its peak area divided by the corresponding peak area of ribitol, which is used as internal standard. All known artifact peaks, such as peaks due to column bleed and MSTFA artifact peaks, were not considered in the final data analyses. Integrated peak areas of multiple derivative peaks belonging to the same compound were summed and considered as single compound. Each sample was characterized by the same number of variables and each of these variables was represented across all observations with the same sequence. Thus, a data matrix was generated by intensities of the commensal peaks from all samples to characterize the biochemical pattern of each sample. The obtained matrix was then employed for correlation analysis and pattern recognition.

For testing the precision and accuracy, four derivatized samples from one same case were consecutively injected into the GC system. The stability of retention time was of great benefit for matching and extracting the coeluting peaks. In addition, the technical replicates were performed for three times.

2.5. Data processing and pattern recognition

After GC/MS analysis, each sample was represented by a GC/MS TIC, and the peak areas of compounds were integrated. The peak area ratio of each compound to a corresponding internal standard was calculated as the response. Statistical analysis was performed using a two sample *t*-test. The differentially expressed compounds with *P*-values of <0.05 were considered statistically significant. Principal component analysis (PCA) was used to differentiate the samples and performed in the MATLAB software (version 7.2, MathWorks, USA) [22]. The classification performance (specificity and sensitivity) of samples was assessed by the area under the curve (AUC) of the receiver–operating characteristic (ROC) curves.

3. Results and discussion

3.1. Study population

The clinicopathological characteristics of the oesophageal cancer patients are summarized in Table 1. As listed in Table 1, 20 oesophageal cancer patients were enrolled to constitute the study

Table 1
Clinicopathologic characteristics of oesophageal cancer patients in this study.

Patient no.	Sex/age (years)	Histology	Pathologic grade[a]	Stage	Lymph node metastasis
1	F/54	ESCC	PD	IIa	N0
2	M/62	ESCC	MD	III	N1
3	M/63	ESCC	MD	III	N0
4	F/69	ESCC	MD	IIa	N0
5	M/45	ESCC	PD	III	N1
6	M/70	ESCC	PD	IIa	N0
7	F/41	ESCC	MD	IIa	N0
8	M/60	ESCC	PD	III	N1
9	M/56	ESCC	MD	I	N0
10	M/64	ESCC	PD	III	N1
11	M/42	ESCC	MD	IIa	N0
12	F/54	Adenocarcinoma	MD	IIa	N0
13	M/54	ESCC	MD	IIa	N0
14	M/43	ESCC	PD	IIa	N0
15	M/51	ESCC	PD	III	N1
16	M/57	ESCC	MD	IIa	N0
17	M/58	ESCC	MD	IIa	N0
18	F/76	Adenocarcinoma	MD	IIa	N0
19	M/61	ESCC	PD	III	N0
20	M/66	ESCC	P	III	N1

[a] PD, poorly differentiated; MD, moderately differentiated.

population (15 males and 5 females; age range, 41–76 years; mean age, 57.3 years; median age, 57.5 years) and the paired tissue specimens were collected for GC/MS study. Disease staging was determined according to the American Joint Committee on Cancer (AJCC) for esophageal tumors. All patients were subjected to surgical resection of the primary tumor and dissection of lymph nodes. Tumor size, lymph node numbers, differentiation status, and lymphovascular invasion were also evaluated.

3.2. Metabolomic profiling of samples

Representative GC/MS TIC chromatograms of samples from the control group and study group were displayed in Fig. 1. In the GC/MS TIC chromatograms of tissue samples from the study and control groups, the majority of the peaks were identified as endogenous metabolites based on NIST mass spectra library, including amino acids, organic acids, carbohydrates and fatty acids. These metabolites were known to be involved in multiple biochemical processes, especially in energy and lipid metabolism [23]. There were 84 signals obtained. Table 2 shows the 67 signals which could be auto-identified by the NIST library through comparison their fragmentation patterns composed of all the fragment ions with a standard mass chromatogram. The remaining 17 peaks which could not be identified by the NIST library were not listed. The resulting data consisted of peak number, retention time, material name, and ion intensity. The first three fragment-ion m/z values with the highest abundance within each fragmentation pattern and the matching percentage to the NIST library were also listed in Table 2. All the amino acids in the "84 metabolite-panel" were further identified through correlation with retention times and fragmentation patterns when compared with the corresponding commercially available standards.

Four TIC profiles of consecutively injected samples of the same aliquot were presented (Fig. 2), and the data showed stable retention time with no drift in all of the peaks. The consistency of sample injection was important for obtaining stable TICs, reflecting the stability of GC/MS analysis and reliability of the metabolomic data. Furthermore, the sample preparation was quite consistent for the samples as evidenced by the triplicates of the same case.

After normalization of data, marker metabolites that were responsible for the separation of the tumor group from the control group were summarized in Table 3. Except for L-altrose, D-galactofuranoside, arabinose, and bisethane which were found to be present at higher levels in the control group, the remaining marker metabolites were found in a larger amount in the tumor group. The levels of all metabolites were found to be statistically different between the two groups ($P < 0.05$).

3.3. Pattern recognition and function analysis

PCA, an unsupervised projection method used to visualize the dataset and display the similarity and difference, was performed [10,14,24,25]. The PCA scores plot showed the two groups were scattered into two different regions (Fig. 3(a)). A secondary PCA model was constructed using the marker metabolite intensities as variables. ROC analysis using the cross-validated predicted Y (predicted class) values was performed to validate the robustness of the PCA model in discriminating tumor from the control. The sensitivity and specificity trade-offs were summarized for each variable using the area under the ROC denoted as AUC, which of this PCA model was 1 (Fig. 3(b)). The high AUC value of the respective ROC analyses confirmed that the PCA model with the combination of the three principal components gave a good discriminating value. Of note, the intension for this analysis was not to replace the established histopathologic evaluation of oesophageal cancer, rather to identify metabolites that hold the potential to augment the metabolic biomarkers gleaned from histologic findings, as routine histopathology provides no molecular characteristics on the biopsied specimens.

Among the selected markers, we found that some of them were worthy of further investigation. We would like to discuss their roles during the process of tumor metabolism associated with oesophageal cancer.

Valine, an essential amino acid, was implicated in the distinctive metabolomic profile of human esophageal tumors. It is worth noting that increased valine level was also found in hepatocellular carcinoma, due to an increased glycolysis [18]. In hepatocellular carcinoma, a direct inhibitory effect on tumor growth was confirmed after the depletion of valine [26,27]. The level of isoleucine, a branched-chain amino acid, was also found to be higher in the oesophageal cancer group than the control group. Valine and isoleucine share the same enzyme systems (branched-chain amino acid transferase and branched-chain alpha-ketoacid dehydrogenase for their initial degradative steps), which are considered as a group in terms of their roles in amino acid homeostasis [28]. Malignant transformation and tumor progression are often accompanied

Table 2
Metabolites of the oesophageal cancer and paired tissue[a].

Peak no.	Retention time	Metabolites	*m*/*z* no. 1	*m*/*z* no. 2	*m*/*z* no. 3	Match percent (%)
1	5.73	Acetic acid	73	147	66	85
3	6.53	Silanamine	171	73	186	87
4	6.71	Propenoic acid	147	73	217	86
5	7.05	Bisethane	147	73	103	84
7	8.83	Propanoic acid	147	73	117	90
8	9.18	Butanoic acid	73	147	191	72
9	9.30	L-Valine	73	144	218	91
10	9.76	L-Alanine	116	73	147	86
11	10.12	Glycine	174	73	147	80
12	10.32	Butanoic acid	73	131	147	80
14	10.78	Benzyl alcohol	91	165	135	96
15	10.84	Butanamine	73	147	217	87
16	11.03	Butanoic acid	147	73	117	91
17	11.05	Furandicarboxylic acid	285	73	147	91
18	11.29	Isoleucine	73	218	158	87
19	11.40	Phosphate	155	199	211	80
20	11.47	Phosphoric acid	211	133	255	92
23	12.71	Urea	147	189	73	94
24	13.06	Serine	204	73	218	94
25	13.40	L-Leucine	158	73	147	91
26	13.51	Phosphate	299	73	314	96
28	14.71	Pyrimidine	241	99	255	93
29	14.82	Butenedioic acid	245	73	147	86
31	15.91	L-Threonine	73	218	117	91
32	16.67	Aminoquinoline	160	131	116	85
33	19.00	Malic acid	73	147	233	91
34	19.77	L-Methionine	176	73	128	72
35	19.83	L-Proline	156	73	147	78
36	20.03	L-Aspartic acid	232	73	100	80
37	20.12	Naphthalene	84	174	73	90
38	20.41	Hexadecanoic acid	73	299	120	75
39	20.93	Creatinine	73	115	143	93
40	21.03	L-Cysteine	73	220	147	84
43	24.39	L-Asparagine	73	116	231	89
44	25.06	L-Phenylalanine	218	73	192	72
45	25.28	L-Lysine	84	73	156	91
46	25.55	Aminoadipic acid	73	260	147	72
47	26.14	Ribitol	73	217	147	92
48	26.91	Glutamine	156	73	245	78
49	26.98	Glycerophosphoric acid	73	299	357	86
50	27.48	Purine	265	73	280	95
52	28.22	Octanoic acid	73	273	147	91
53	28.30	Tetradecanoic acid	73	117	285	84
54	28.56	Arabinofuranoside	73	217	147	72
55	28.85	Glucofuranose	217	73	127	83
57	29.22	Tyrosine	179	73	208	91
58	29.92	Galactopyranose	204	73	191	93
61	30.91	Gulonic acid	73	205	147	70
62	30.97	L-Ascorbic acid	73	332	147	93
63	31.43	L-Altrose	217	73	147	72
64	31.85	D-Glucose	204	73	217	87
65	32.05	Arabinose	73	217	191	74
67	32.36	Hexadecanoic acid	313	117	73	97
68	33.46	D-Galactofuranoside	217	73	147	73
69	33.74	Myo-inositol	73	305	217	81
70	33.81	Naphthalenepentanoic acid	305	191	320	93
72	35.41	Octadecadienoic acid	75	117	129	85
73	35.51	Oleic acid	117	73	339	76
74	35.67	Naphthalene	314	161	134	70
75	35.98	Octadecanoic acid	341	117	73	98
76	36.11	D-Ribofuranose	73	299	147	72
77	39.60	Myo-inositol	73	318	217	81
80	41.79	Mannoonic acid	73	217	147	75
81	43.56	Gulose	204	73	361	74
82	45.06	Lyxopyranose	217	207	73	82
83	47.28	Benzoic acid	119	193	73	85
84	49.28	Cholesterol	129	329	368	99

[a] Peaks in the TICs are numbered according to their retention time. The identification of metabolite is based on NIST mass spectra database according to the match of masses (*m*/*z*) between the interested peak's fragmentation pattern and that from the standard database.

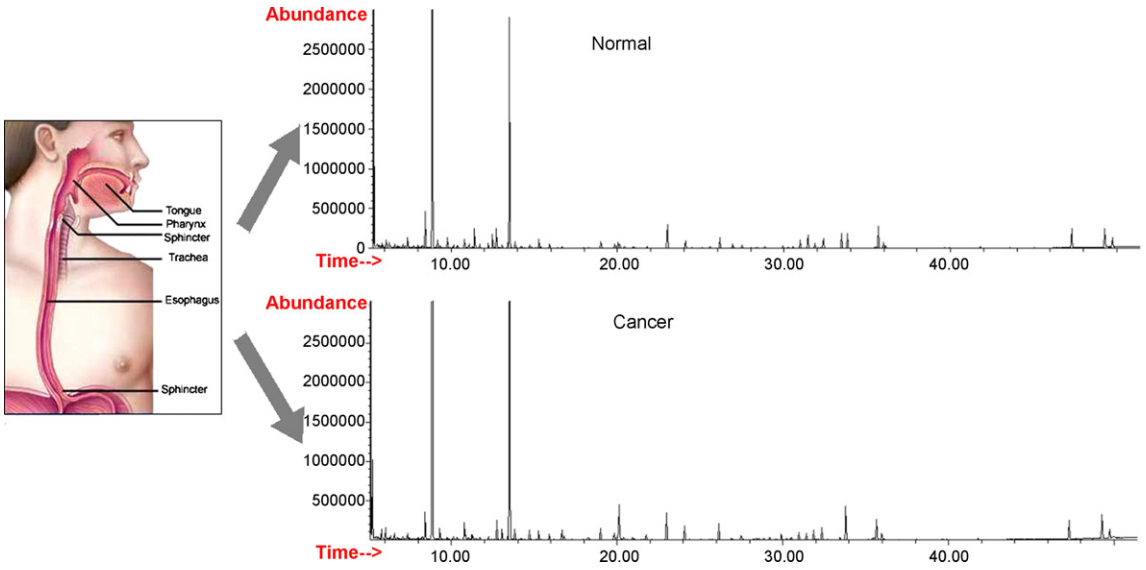

Fig. 1. Representative GC/MS total ion chromatograms of the samples from the two groups (oesophageal cancer and normal mucosae) after chemical derivatization.

by structural changes in carbohydrate components of glycoproteins and glycolipids. Studies with tumor cell glycosylation mutants and specific inhibitors of glycosylation suggest that expression of sialylated and beta (1-6) branched asparagine-linked oligosaccharides are required for tumor cell invasion and metastasis [29]. Furthermore, the change in asparagine metabolism is probably related to low affinity with L-type amino acid transporter 1 in tumor cell lines [30]. In this study, an increased level of alanine and serine was also found in oesophageal cancer samples, suggesting involvement of glycolysis.

In the current study, the level of tyrosine (Tyr) was higher in the oesophageal cancer group than that in the control group in our study. Tyr is synthesized from the essential amino acid phenylalanine (Phe). The conversion of Phe to Tyr is catalyzed by the enzyme phenylalanine hydroxylase, a monooxygenase. All free amino acids are essential metabolic substrates for tumor cells. Solid tumors exhibit relatively specific amino acid dependency that functionally regulates their survival, proliferation, and metastasis. It has been reported that human A375 and murine B16 melanoma cells are tyrosine (Tyr)4/phenylalanine (Phe)-dependent [31]. Moreover, Tyr/Phe restriction also inhibits invasion and metastasis of other cancers [32,33]. Specific amino acid dependency is one of the metabolic abnormalities of cancer cells and can also be regarded as the metabolic basis for their malignant behavior. We speculated that there was some relationship between the altered level of Tyr and oesophageal cancer metabolism.

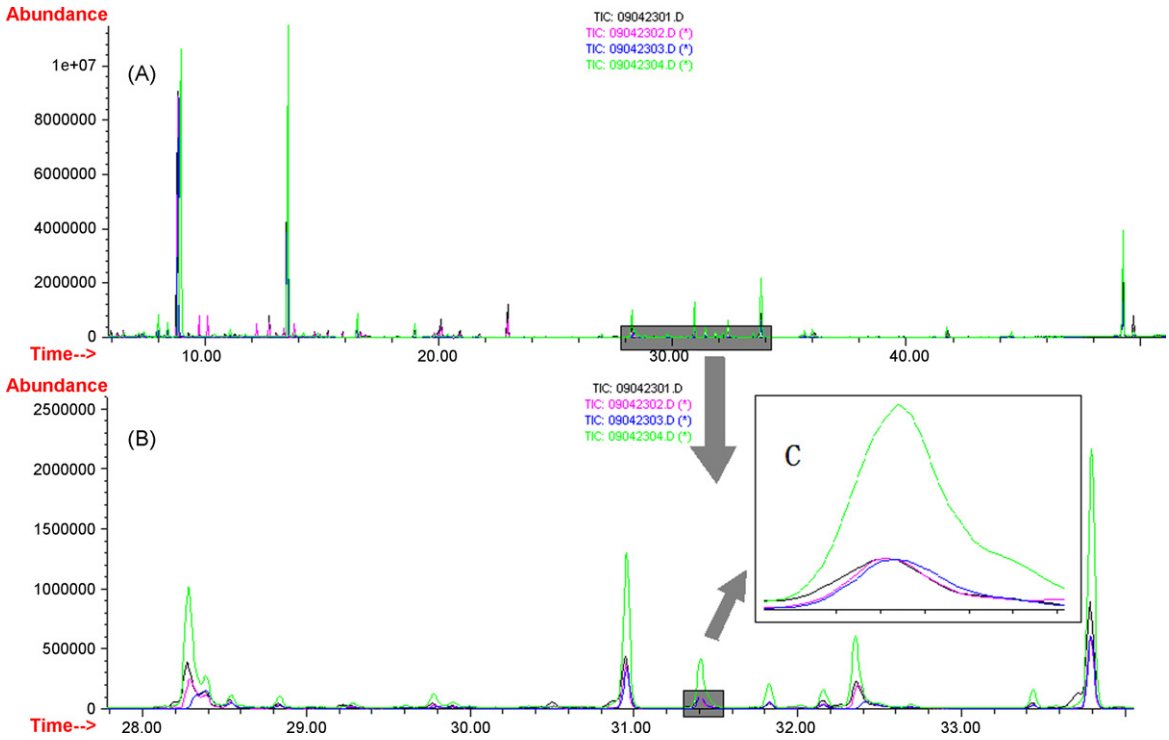

Fig. 2. The overlay chromatograms of four parallel samples for the validation of precision. (A) The total ion current chromatogram of GC–MS analysis; (B) enlarged part of TIC chromatogram from 11 to 15 min; (C) zoomed in response of one representative peak with small area.

Table 3
Marker metabolites found in GC/MS chromatograms of the two groups.

Metabolite	Rt (min)	Chemical class	*P*-value[a]
L-Valine	9.30	Amino acid	0.000000004
Naphthalene	20.12	Others	0.000000045
1-Butanamine	10.84	Others	0.000000053
L-Altrose	31.43	Carbohydrates	0.000000073
D-Galactofuranoside	33.46	Carbohydrates	0.000000196
Pyrimidine	14.71	Pyrimidine nucleoside	0.000000543
Aminoquinoline	16.67	Others	0.000001410
L-Tyrosine	29.22	Amino acid	0.000001681
Isoleucine	11.29	Amino acid	0.000002688
Purine	27.48	Purine nucleoside	0.000013755
Serine	13.06	Amino acid	0.000023238
Phosphoric acid	11.47	Inorganic acid	0.000029045
Myo-inositol	39.6	Others	0.000032629
Arabinose	32.05	Carbohydrates	0.000071416
Arabinofuranoside	28.56	Carbohydrate	0.000309028
L-Asparagine	24.39	Amino acid	0.000647234
Tetradecanoic acid	28.3	Fatty acid	0.001811760
L-Alanine	9.76	Amino acid	0.002016721
Hexadecanoic acid	20.41	Fatty acid	0.007699254
Bisethane	7.05	Others	0.008971290

[a] Statistical *P*-value calculated using a two sample *t*-test (significance at $P < 0.05$).

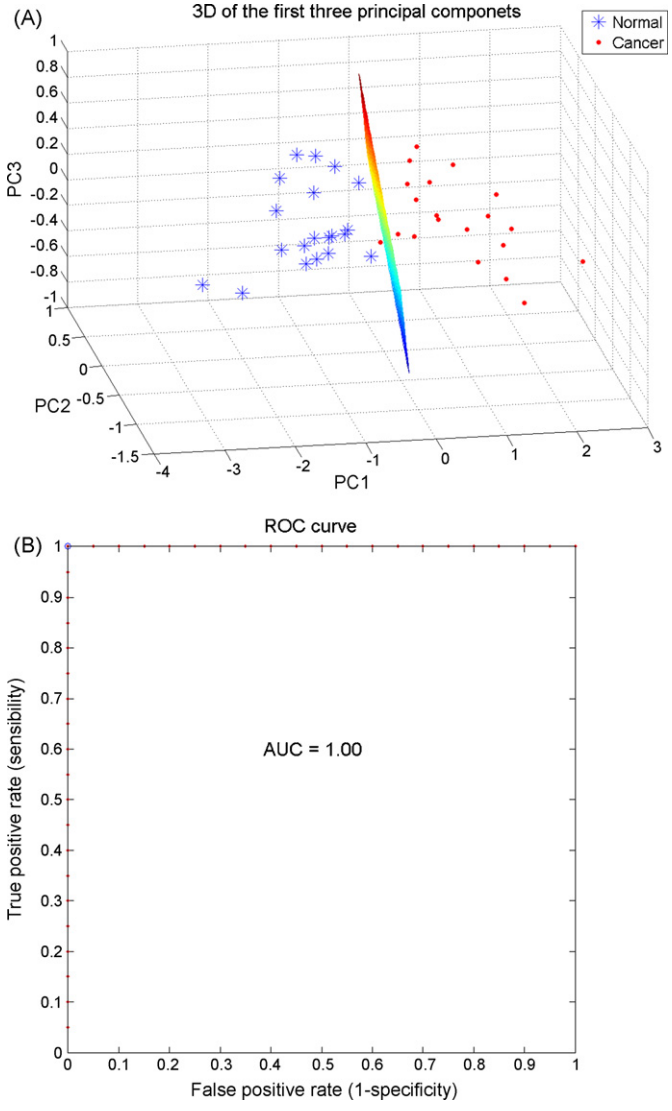

Fig. 3. (A) PCA scores plot discriminating esophageal tumor specimens from control specimens based on GC/MS marker metabolites. (B) ROC curve determined using the cross-validated predicted *Y*-values of the GC/MS PCA model.

Hexadecanoic acid and tetradecanoic acid are common fatty acids in human. In cancer cells, fatty acid synthase is active, leading to transcriptionally up-regulated fatty acid synthesis [34]. The same event takes place in hepatoma cells and serum of liver cancer patients [11,35]. An early study demonstrated that polyunsaturated fatty acids were increased in BT4C gliomas in rats during therapy-induced apoptosis [36]. A change in the metabolism of fatty acids in tumor cells could lead to the pathogenesis of cancer [37]. Therefore, we added hexadecanoic acid and tetradecanoic acid into our diagnostic model for oesophageal cancer.

The change in carbohydrates metabolism probably resulted from promotion of glycolysis and disruption of tricarboxylic acid cycle (TCA cycle). Perturbations of liver metabolism by liver toxins caused an increase in glycogenolysis and/or a decrease in glycogen reduction [38,39], and a decreased level in glucose and glycogen also was found in hepatoma and colorectal cancer [18,40]. Based on the findings of our current study, we speculate that abnormal metabolism of carbohydrates may be associated with tumor growth with its large energy requirement from aggressive cell proliferation. As substrates and nitrogen sources, the alteration in primidine and purine as shown in our study was probably associated with the higher propagation rate of the tumor cells.

4. Conclusions

Our work is an integrated analysis based on metabolomic profiling of biopsied tissues by chemical derivatization and gas chromatography/mass spectrometry in oesophageal cancer patients. Gas chromatography/mass spectrometry was proved to be a feasible and complementary analytical platform for tissue metabolic typing in terms of its high sensitivity and reproducibility. The multivariate analysis of metabolomic data including the 20-marker metabolites established an optimized diagnostic model to discriminate tumor from normal mucosae with AUC of 1, suggesting that metabolomics may be useful for clinical diagnosis and in delineating carcinogenesis pathways in oesophageal cancer.

Acknowledgements

This study was financially supported by National Basic Research Program of China (2007CB936000), Ministry of Health (2009ZX10004-301), China National Key Projects for Infectious Diseases (2008ZX10002-017) and National Nature Science Foundation of China (No. 30772505 & No. 30872503).

References

[1] F. Kamangar, G.M. Dores, W.F. Anderson, J. Clin. Oncol. 24 (2006) 2137.
[2] P. Bytzer, P.B. Christensen, P. Damkier, K. Vinding, N. Seersholm, Am. J. Gastroenterol. 94 (1999) 86.
[3] S.S. Devesa, W.J. Blot, J.F. Fraumeni Jr., Cancer 83 (1998) 2049.
[4] J.A. Ajani, J. Clin. Oncol. 23 (2005) 4256.
[5] M. Wakatsuki, Y. Suzuki, S. Nakamoto, T. Ohno, H. Ishikawa, H. Kiyohara, M. Kiyozuka, K. Shirai, Y. Nakayama, T. Nakano, J. Gastroenterol. Hepatol. 22 (2007) 715.
[6] M. Groome, J. Lindsay, P.E. Ross, J.P. Cotton, T.R. Hupp, J.F. Dillon, Eur. J. Gastroenterol. Hepatol. 20 (2008) 961.
[7] A.A. Evans, G. Chen, E.A. Ross, F.M. Shen, W.Y. Lin, W.T. London, Cancer Epidemiol. Biomarkers Prev. 11 (2002) 369.
[8] W.M. Claudino, A. Quattrone, L. Biganzoli, M. Pestrin, I. Bertini, A. Di Leo, J. Clin. Oncol. 25 (2007) 2840.
[9] W.R. Wikoff, J.A. Gangoiti, B.A. Barshop, G. Siuzdak, Clin. Chem. 53 (2007) 2169.
[10] J. Yang, G. Xu, Q. Hong, H.M. Liebich, K. Lutz, R.M. Schmulling, H.G. Wahl, J. Chromatogr. B Analyt. Technol. Biomed. Life Sci. 813 (2004) 53.
[11] R. Xue, Z. Lin, C. Deng, L. Dong, T. Liu, J. Wang, X. Shen, Rapid Commun. Mass Spectrom. 22 (2008) 3061.
[12] M. Bogdanov, W.R. Matson, L. Wang, T. Matson, R. Saunders-Pullman, S.S. Bressman, M. Flint Beal, Brain 131 (2008) 389.
[13] J. Chen, X. Zhao, J. Fritsche, P. Yin, P. Schmitt-Kopplin, W. Wang, X. Lu, H.U. Haring, E.D. Schleicher, R. Lehmann, G. Xu, Anal. Chem. 80 (2008) 1280.

[14] H. Wu, R. Xue, L. Dong, T. Liu, C. Deng, H. Zeng, X. Shen, Anal. Chim. Acta 648 (2009) 98.
[15] J.K. Nicholson, J. Connelly, J.C. Lindon, E. Holmes, Nat. Rev. Drug Discov. 1 (2002) 153.
[16] J.C. Lindon, E. Holmes, M.E. Bollard, E.G. Stanley, J.K. Nicholson, Biomarkers 9 (2004) 1.
[17] J. Yang, G. Xu, Y. Zheng, H. Kong, T. Pang, S. Lv, Q. Yang, J. Chromatogr. B Analyt. Technol. Biomed. Life Sci. 813 (2004) 59.
[18] E.C. Chan, P.K. Koh, M. Mal, P.Y. Cheah, K.W. Eu, A. Backshall, R. Cavill, J.K. Nicholson, H.C. Keun, J. Proteome Res. 8 (2009) 352.
[19] C.Y. Lin, H.F. Wu, R.S. Tjeerdema, M.R. Viant, Metabolomics 3 (2007) 55.
[20] H.K. Kim, Y.H. Choi, T.J. Luijendijk, R.A. Rocha, R. Verpoorte, Phytochem. Anal. 15 (2004) 257.
[21] R. Xue, L. Dong, H. Wu, T. Liu, J. Wang, X. Shen, Clin. Chem. Lab. Med. (2009) [Epub ahead of print].
[22] J. Trygg, E. Holmes, T. Lundstedt, J. Proteome Res. 6 (2007) 469.
[23] C. Postic, R. Dentin, J. Girard, Diabetes Metab. 30 (2004) 398.
[24] M.L. Anthony, V.S. Rose, J.K. Nicholson, J.C. Lindon, J. Pharm. Biomed. Anal. 13 (1995) 205.
[25] O. Beckonert, M.E. Bollard, T.M.D. Ebbels, H.C. Keun, H. Antti, E. Holmes, J.C. Lindon, J.K. Nicholson, Anal. Chim. Acta 490 (2003) 3.
[26] K. Taniguchi, T. Nonami, A. Nakao, A. Harada, T. Kurokawa, S. Sugiyama, N. Fujitsuka, Y. Shimomura, S.M. Hutson, R.A. Harris, H. Takagi, Hepatology 24 (1996) 1395.
[27] K. Ishigure, Y. Shimomura, T. Murakami, T. Kaneko, S. Takeda, S. Inoue, S. Nomoto, K. Koshikawa, T. Nonami, A. Nakao, Clin. Chim. Acta 312 (2001) 115.
[28] A.M. Landel, W.G. Hammond, M.M. Meguid, Cancer 55 (1985) 230.
[29] J.W. Dennis, S. Laferte, S. Yagel, M.L. Breitman, Cancer Cells 1 (1989) 87.
[30] O. Yanagida, Y. Kanai, A. Chairoungdua, D.K. Kim, H. Segawa, T. Nii, S.H. Cha, H. Matsuo, J. Fukushima, Y. Fukasawa, Y. Tani, Y. Taketani, H. Uchino, J.Y. Kim, J. Inatomi, I. Okayasu, K. Miyamoto, E. Takeda, T. Goya, H. Endou, Biochim. Biophys. Acta 1514 (2001) 291.
[31] Y.M. Fu, G.G. Meadows, J. Nutr. 137 (2007) 1591S.
[32] Y.M. Fu, Z.X. Yu, Y.Q. Li, X. Ge, P.J. Sanchez, X. Fu, G.G. Meadows, Nutr. Cancer 45 (2003) 60.
[33] B.A. Pelayo, Y.M. Fu, G.G. Meadows, Int. J. Oncol. 18 (2001) 877.
[34] F.P. Kuhajda, Cancer Res. 66 (2006) 5977.
[35] A.I. Cederbaum, E. Rubin, Cancer Res. 36 (1976) 2274.
[36] J.L. Griffin, K.K. Lehtimaki, P.K. Valonen, O.H. Grohn, M.I. Kettunen, S. Yla-Herttuala, A. Pitkanen, J.K. Nicholson, R.A. Kauppinen, Cancer Res. 63 (2003) 3195.
[37] R.K. Ockner, R.M. Kaikaus, N.M. Bass, Hepatology 18 (1993) 669.
[38] H. Wu, X. Zhang, X. Li, Y. Wu, F. Pei, Anal. Biochem. 339 (2005) 242.
[39] N.J. Waters, E. Holmes, C.J. Waterfield, R.D. Farrant, J.K. Nicholson, Biochem. Pharmacol. 64 (2002) 67.
[40] Y. Yang, C. Li, X. Nie, X. Feng, W. Chen, Y. Yue, H. Tang, F. Deng, J. Proteome Res. 6 (2007) 2605.